Occupation sites and valence states of Co dopants in (La, Co)-codoped M-type Sr ferrite: ^{57}Fe and ^{59}Co nuclear magnetic resonance studies

H. Sakai, T. Hattori, Y. Tokunaga, S. Kambe, H. Ueda, Y. Tanioku, C. Michioka, K. Yoshimura, K. Takao, A. Shimoda, T. Waki, Y. Tabata, and H. Nakamura

Phys. Rev. B **98**, 064403 — Published 2 August 2018

DOI: 10.1103/PhysRevB.98.064403

Occupation sites and valence states of Co dopants in (La, Co)-codoped M-type Sr ferrite: ^{57}Fe and ^{59}Co nuclear magnetic resonance studies

H. Sakai,* T. Hattori, Y. Tokunaga, and S. Kambe
Advanced Science Research Center, Japan Atomic Energy Agency, Tokai, Ibaraki, 319-1195, Japan.

H. Ueda, Y. Tanioku, C. Michioka, and K. Yoshimura
Department of Chemistry, Graduate School of Science, Kyoto University, Kyoto 606-8502, Japan

K. Takao, A. Shimoda, T. Waki, Y. Tabata, and H. Nakamura†
Department of Materials Science and Engineering, Kyoto University, Kyoto 606-8501, Japan
(Dated: July 20, 2018)

To specify preferential occupation sites of Co substituents and to clarify charge and spin states of Co ions in (La, Co)-cosubstituted hexagonal magnetoplumbite-type (M-type) Sr ferrite $Sr_{1-x}La_xFe_{12-y}Co_yO_{19}$ ($x, y \leq 0.4$), ^{57}Fe and ^{59}Co nuclear magnetic resonance (NMR) spectra are measured under zero and external magnetic fields using powdered and single crystalline specimens. For comparison, NMR investigations of non-doped and La- or Co-doped M-type Sr ferrites are also performed. Ferrimagnetic M-type Sr ferrite contains the following five crystallographic Fe sites: the majority spin sites $12k$, $2a$, and $2b$, and the minority spin sites $4f_1$ and $4f_2$. Based on ^{57}Fe and ^{59}Co NMR, a plausible model of (La, Co)-codoped Sr ferrite is deduced. To a considerable degree, the charge compensation between La^{3+} and Co^{2+} works in the equal (La, Co)-codoped case, where more than half of the Co ions are considered to be present in the minority spin $4f_1$ sites at the center of the oxygen tetrahedra, with the S=3/2 state carrying a small orbital moment owing to spin-orbit interaction. The remaining small number of high-spin Co^{2+} (S=3/2, L=1) ions with unquenched orbital moments would be distributed to the other octahedral $12k$, $2a$, and $4f_2$ sites.

I. INTRODUCTION

Slight doping of elements into semiconductors, magnets, or superconductors is often performed to achieve functional improvements. In general, it is nontrivial to identify the occupation sites and valence states of transition metal dopants, which are distributed sparsely throughout a base compound. If this role of dopants is clarified at the microscopic level, a beneficial direction can be indicated for further improvements.

Hexagonal magnetoplumbite-type (M-type) strontium ferrite $SrFe_{12}O_{19}$ is widely used as a base material for permanent magnets owing to its excellent cost performance and high chemical stability.[1] In M-type Sr ferrite, slight substitution of transition-metal element Co for Fe is known to improve the material's performance as a hard magnet. Simultaneously, the same amount of rare earth element La can be substituted empirically at the Sr sites for charge compensation, i.e., assuming $(Sr^{2+}\text{-}La^{3+})(Fe^{3+}\text{-}Co^{2+})_{12}O_{19}$.[2] This ionic charge model should be re-examined because previous Mössbauer spectroscopy results[3,4] have suggested the existence of divalent Fe^{2+} ions in a (La, Co)-cosubstituted M-type Sr ferrite. The assigned Fe^{2+} spectra, however, have not been observed in recent Mössbauer spectroscopy study using single crystals.[5] In a recent solid solution investigation[6] of Sr–La–Co–Fe–O, it has been suggested that the amount of La dopants is not necessarily equal to that of Co dopants. Systematic attempts at single crystal growth[7,8] suggest that the amounts of La and Co dopants tend to deviate from the nominal ratio of La:Co=1:1. In other words, the charge compensation between La^{3+} and Co^{2+} is not always perfect. Moreover, the preferred sites for Co substitution remain under debate, as described below.

The crystal structure of M-type Sr ferrite is shown in Fig. 1. It contains the following five crystallographic Fe sites: $2a$, $2b$, $4f_1$, $4f_2$, and $12k$ sites in Wyckoff notation, as listed together with their respective local oxygen coordination in Table I. The magnetic structure is ferrimagnetic with a saturation moment of 20 μ_B per formula unit (f.u.) in the ground state, where the moments of 5 μ_B for high-spin Fe^{3+} (d^5) are aligned along the c axis at the majority spin sites of $2a$, $2b$ and $12k$ and in the opposite direction at the minority spin sites of $4f_1$ and $4f_2$, as summarized in Table I.

As for the Co sites in (La, Co)-codoped M-type Sr ferrites, the results of a previous combined Raman and Mössbauer study[9] indicated that Co atoms preferentially occupy octahedral $4f_2$ (and possibly $2a$) sites. However, this conclusion was found to disagree with the combined result of neutron diffraction (ND) and extended X-ray absorption fine structure (EXAFS) spectra[10], which excluded substitutions at the $4f_2$ and $2b$ sites. Furthermore, Co substitutions at the $4f_1$ site were suggested from ND[11], NMR[3] and X-ray magnetic circular dichroism (XMCD)[10] measurements, while another NMR research[12] suggested a different possibility of simultaneous occupation of the $4f_1$ and $4f_2$ sites. Given that the assignments of ^{57}Fe Mössbauer spectra[3,4,9] have been confirmed by recent first-principle calculations[13,14] by using the density functional theory, the discrepancies in the possible Co substitution sites may not be caused by incorrect assignments of Fe sites, but possibly by differences in chemical compositions, sample shapes and/or

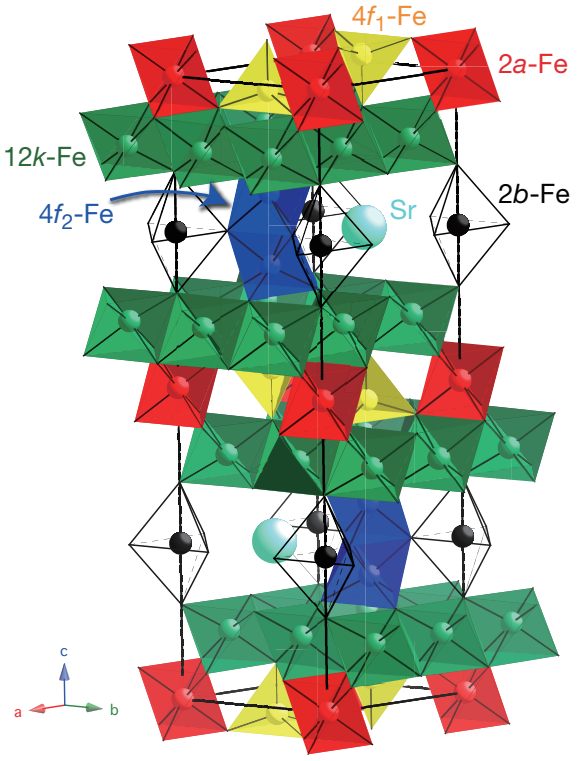

FIG. 1. Crystal structure of M-type Sr ferrite $SrFe_{12}O_{19}$ (hexagonal, $P6_3/mmc$). Oxygen atoms, which are at the corner of each polyhedron, are omitted for clarity. Each iron atom is located at the center of a polyhedron. The five crystallographic iron sites are labelled by their Wyckoff notation.

particle size between the respective experimental investigations.

Progress toward solving this intricate assignment issue has been achieved in a very recent ^{59}Co NMR study[15] over a wide frequency range by using chemically well-characterized single crystals of (La, Co)-cosubstituted M-type Sr ferrite, in which low-frequency resonances around 80 MHz and high-frequency resonances above 250 MHz were observed simultaneously. Notably, the respective resonances were reported independently in early studies: ^{59}Co NMR around 80 MHz by M. W. Pieper *et al.*[12], and those in the much higher range of 250–600 MHz by K. Kouřil[16]. The simultaneous observation of both low- and high-frequency resonances of ^{59}Co NMR strongly suggests that Co ions are doped into several Fe sites, and/or that various spin and charge states might be possible: high-, low-spin, and divalent or trivalent, as summarized in Table II. The possible combinations of electronic states and Co sites should be re-examined carefully.

To arrive at a consensus on Co site occupations and to understand the electronic states of Co ions, we performed thorough ^{57}Fe and ^{59}Co-NMR measurements of (La, Co)-codoped M-type Sr ferrites, by using chemically well-characterized polycrystalline and single crystal samples.

TABLE I. Crystallographic Fe sites in $SrFe_{12}O_{19}$ with space group $P6_3/mmc$ and relative magnetic moment directions at the sites.

Wyckoff notation	Oxygen coordination	Moment direction
$2a$	Octahedral	↑
$2b$	Bipyramidal	↑
$4f_1$	Tetrahedral	↓
$4f_2$	Octahedral	↓
$12k$	Octahedral	↑

TABLE II. High- and low-spin values of Co^{2+} and Co^{3+}. The low-spin values are given for octahedral, tetrahedral, and bipyramidal symmetries. Tetrahedral Co^{2+} with $e_g^4 t_{2g}^3$ configuration has single spin state of S =3/2 only.

	High spin	Low spin		
		Octa.	Tetra.	Bipyram.
Co^{2+} (d^7)	$\frac{3}{2}$	$\frac{1}{2}$	—	$\frac{1}{2}$
Co^{3+} (d^6)	2	0	1	1

II. EXPERIMENTAL

Polycrystalline samples of (La, Co)-codoped M-type Sr ferrites $Sr_{1-x}La_xFe_{12-y}Co_yO_{19}$ ($x = y$ =0.1, 0.2, and 0.3), denoted as (La, Co)$_{0.1}$, (La, Co)$_{0.2}$, and (La, Co)$_{0.3}$-codoped, as well as solely La-doped $Sr_{1-x}La_xFe_{12}O_{19}$ (x=0.1, 0.2, 0.3, and 0.5), labeled similarly as $La_{0.1}$, $\cdots$, $La_{0.5}$-doped, were synthesized by performing a standard solid state reaction. Single crystals of pure, ($La_{0.24}$, $Co_{0.11}$), and ($La_{0.29}$, $Co_{0.15}$)-codoped M-type Sr ferrites were prepared using the NaO-flux method,[7] in addition to solely Co-doped $SrFe_{11.93}Co_{0.07}O_{19}$, which is labeled $Co_{0.07}$-doped. Typical size of single crystals was 3×3×0.2 mm^3, in which hexagonal shapes were seen in surface. The (La, Co)$_{0.4}$-codoped single crystals were grown using the traveling solvent floating zone (TSFZ) technique.[8,17] The (La, Co)$_{0.4}$-codoped crystal with a dimension of 2×2×1.8 mm^3 was used for NMR measurement. The compositions were examined using scanning electron microscopy/wavelength dispersive X-ray (SEM-WDX) analysis and inductively coupled plasma atomic emission spectroscopy (ICP-AES).

Powdered specimens for NMR measurements were prepared by coarsely grinding polycrystals or single crystals. The powders were insulated and fixed with varnish in polyimide tubes. For single crystal NMR measurements, instead of the polyimide tube filled with the powdered sample, one piece or several pieces of crystals placed on platforms made of glass or glass-epoxy were inserted into the NMR coils. The typical dimensions of the crystals in the hexagonal plane were several millimeters, and in the direction of the c-axis, they ranged between 50 μm and several millimeters. The NMR probe was loaded into a ^{4}He cryostat.

^{57}Fe nuclei with nuclear spin $I = 1/2$ and small natural abundance of 2.19% have a very low gyromagnetic ratio (γ_N) of 0.135758 MHz/kOe. In ferro(ferri-)magnets, however, rf fields (H_1) of the nuclear spin excitation are effectively enhanced owing to electronic spin oscillations, resulting in an enhancement factor of ∼10–100 or owing to magnetic domain wall motion, resulting in an enhancement factor of 10^3–10^4 to the 'bare' H_1. This so-called H_1 enhancement and huge internal fields of ∼400–600 kOe of these compounds enable us to perform ^{57}Fe NMR measurements under zero external field. On the other hand, ^{59}Co nuclei with $I = 7/2$ and natural abundance of 100% have a relatively larger $\gamma_N = 1.0054$ MHz/kOe, which enabled us to observe ^{59}Co-NMR of dilute dopants in the doped systems.

NMR measurements were carried out using a phase-coherent, pulsed spectrometer capable of measurement over the frequency range of 0.5–500 MHz. All the NMR data were taken at the temperature (T) of 4.2 K. NMR spectra were recorded by sweeping the frequency in the tuned rf network at each point. To form the nuclear spin echoes, 90°–180°conditions were used with a first pulse duration of 2–3 μs, where the rf power of the nuclear excitation was optimized at each NMR spectral peak. The separation τ between the first and the second pulses was typically 10–20 μs, as short as possible. The pulse repetition interval of 50 ms was used for NMR signal accumulations. The obtained spin-echo intensities were divided by the cube of circuit frequencies (ν^3) in order to compensate the frequency-dependent enhancement factor. External magnetic fields were applied using a homogeneous superconducting magnet specified for NMR, to measure the external field dependence of NMR spectra.

III. RESULTS

A. Non-doped $SrFe_{12}O_{19}$

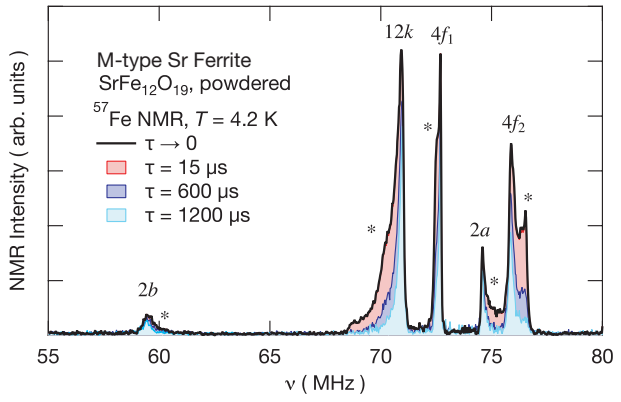

FIG. 2. Frequency-swept ^{57}Fe NMR spectra for powdered M-type Sr ferrite under zero field, which are taken with several separations of $\tau = 15$, 600, and 1200 μs. The extrapolated intensities for $\tau \to 0$ are also shown.

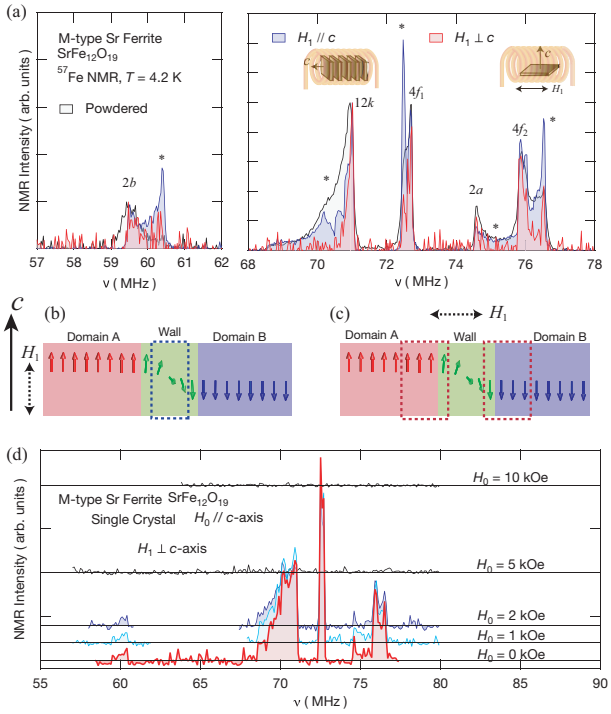

FIG. 3. (a) Frequency-swept ^{57}Fe NMR spectra of single crystals of M-type Sr ferrite under zero field. As schematically illustrated in the insets, two configurations are attempted with the oscillating field of H_1 parallel and perpendicular to the magnetic easy c axis. The NMR intensities are normalized at the peak intensity for the $12k$ sites. Schematic illustrations are also shown for a magnetic domain wall and magnetic domains. The dotted rectangles indicate where NMR can occur for the cases of (b) $H_1 \parallel c$ and (c) $H_1 \perp c$. (d) Frequency-swept ^{57}Fe NMR spectra of single crystal of M-type Sr ferrite in the case of $H_1 \parallel c$ with applying external fields (H_0) along the c axis.

First, let us summarize the ^{57}Fe NMR results of the pure M-type Sr ferrite. Figure 2 shows the ^{57}Fe NMR spectra of a powdered sample of M-type Sr ferrite $SrFe_{12}O_{19}$ under zero field with several separations of $\tau = 15$, 600, and 1200 μs. The NMR peak positions are consistent with those shown in previous studies for M-type Ba and Sr ferrites.[12,13,18–21] The site assignments of the NMR peaks are denoted in Fig. 2. To correct the NMR intensities for the nuclear spin-spin relaxation time T_2 effect, the intensities (I_0) were extrapolated to $\tau \to 0$ assuming a simple Lorentz-type echo decay function of $I_0 \exp(-2\tau/T_2)$. Each NMR peak has an adjoint tail with short T_2, as marked by ($*$) in Fig. 2, which is from the magnetic domain walls.

To confirm that such tail signals correspond to magnetic wall signals, NMR measurements using single crystals were performed additionally, as shown in the inset of Fig. 3(a). Because NMR does not occur if H_1 is applied along the quantization axis of nuclear magnetization, which corresponds to the easy axis of magnetization in this case, NMR intensities in single crystalline magnets

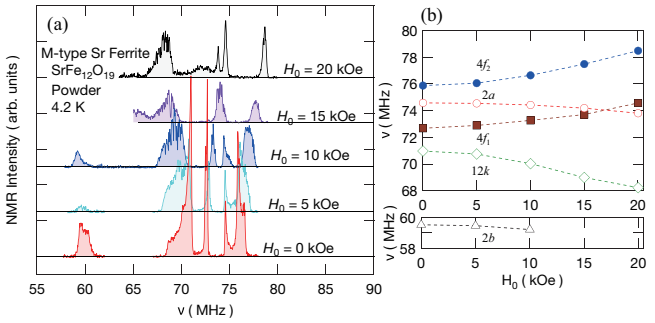

FIG. 4. (a) External field dependence of ^{57}Fe NMR spectra in the powdered M-type Sr ferrite under H_0=0, 5, 10, 15, and 20 kOe. (b) Resonant frequencies versus H_0 plot for the powdered M-type $SrFe_{12}O_{19}$.

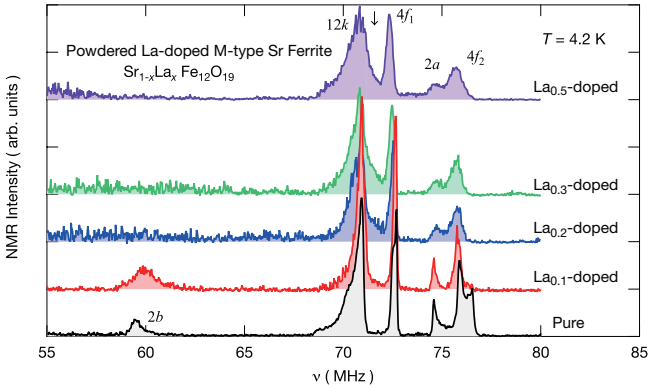

FIG. 5. Zero field ^{57}Fe NMR spectra of powdered polycrystalline $La_{0.1}$, $La_{0.2}$, $La_{0.3}$, and $La_{0.5}$-doped M-type Sr ferrites.

should show a directional dependence on H_1, as schematically illustrated in Figs. 3(b) and (c). In other words, the setting for $H_1 \perp c$ is sensitive to magnetic domains, while that for $H_1 \parallel c$ to magnetic domain walls. It is noted that even in the domain-sensitive setting for the single crystal, as shown in Fig. 3(d), the NMR signals could not be observed if the domain walls were swept out by external field along the c axis. The saturation field along the easy axis for the single crystal is so small as to be of an order of 1 kOe, which is nearly independent of doping levels.[7] The magnetization curves have been measured for single crystals in tabular shapes with typical dimensions of 5×5×0.1 mm^3. Therefore, in this case, the responsible area for the NMR signals were considered to be the domains in the vicinity of domain walls, as indicated in Fig. 3(c). In other words, the ^{57}Fe NMR is caused not from a whole of domains, but from interfacial areas between domains and walls. As can be seen in Fig. 3(a), the NMR intensities denoted by (∗) are always enhanced in the case of $H_1 \parallel c$. Thus, the asymmetric spectral tails in ^{57}Fe NMR originate from the magnetic domain walls.

Figure 4 shows the external field (H_0) dependence of the ^{57}Fe NMR spectra. Given that the hyperfine coupling constant for core-polarization of ^{57}Fe has a negative sign[22], field dependence in case of the majority spin sites shows negative slopes to the external field, while that in case of the minority spin sites shows positive slopes. The observed external field dependence of the ^{57}Fe NMR is very consistent with previous results obtained for M-type Ba and $Pb_{0.7}La_{0.3}$ ferrites.[18,23]

B. Solely La-doped M-type Sr ferrite $Sr_{1-x}La_xFe_{12}O_{19}$

To microscopically investigate the effects of La-Co codoping, it is worthwhile to examine the solely La-doped system beforehand. Figure 5 shows the ^{57}Fe NMR spectra of powdered polycrystalline $La_{0.1}$, $La_{0.2}$, $La_{0.3}$, and $La_{0.5}$-doped M-type Sr ferrites under zero field. As shown in Fig. 5, with La doping, the resonant peak linewidths of the 12k, 4f_1, 2a, and 4f_2 sites expand slightly. Notably, an additional spectral weight appears between the 12k and the 4f_1 peaks with La doping, as denoted by arrow (↓) in Fig. 5. However, the 2b resonance broadens significantly, and appears to be wiped out subsequently owing to low $La_{0.2}$-doping. These can be ascribed to the distributions of hyperfine fields of Fe ions due to different local environments, whose effect should be largest at the Fe 2b sites, which are the closest to the Sr sites. These features are very consistent with the results of previous works on La-substituted M-type Sr ferrite[24]. Here, it is also noted that we could not find the ^{57}Fe-NMR ascribed to Fe^{2+} ions, which should be induced by La^{3+}-doping.

C. Solely Co-doped M-type Sr ferrite $SrFe_{11.93}Co_{0.07}O_{19}$

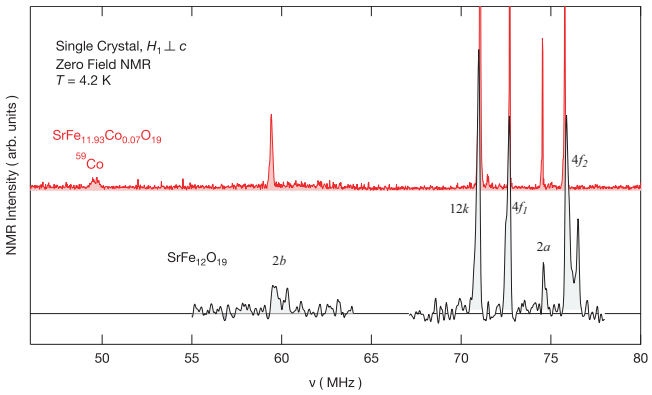

FIG. 6. Frequency-swept ^{57}Fe and ^{59}Co NMR spectra of single crystals of $Co_{0.07}$-doped and non-doped M-type Sr ferrites under zero field with a setting of $H_1 \perp c$.

Here, spectral investigation in the solely Co-doped M-type Sr Ferrite is shown. Owing to the chemical instability of sole Co-doping in M-type Sr ferrite, the lowest upper bound of the amount of Co seems to be $x \sim 0.1$

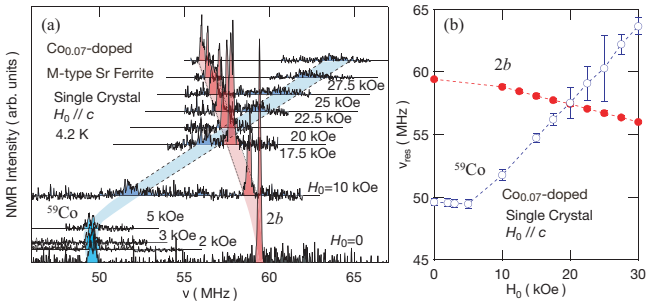

FIG. 7. (a) External field dependence of low-frequency ^{59}Co and 2b-^{57}Fe NMR spectra of a single crystal of $Co_{0.07}$-doped M-type Sr ferrite. The size of single crystal was 5.3×2.1×0.27 mm^3. (b) Resonant frequencies versus H_0 plot.

in $SrFe_{12-x}Co_xO_{19}$. Here, the crystals of $Co_{0.07}$-doped M-type Sr ferrite are available. In this case, the Co ions are firmly trivalent by charge compensation.

Zero field NMR spectra of this crystal are shown in Fig. 6, together with that of non-doped M-type Sr ferrite. The magnitude of H_1 is adjusted to pick up both ^{57}Fe and ^{59}Co NMR signals. The ^{59}Co NMR signal is observed at around 50 MHz as indicated in Fig. 6. The linewidths of ^{57}Fe NMR in the $Co_{0.07}$-doped case are quite sharp as in the non-doped case, although a new small satellite-like peak is seen on the right hand side of the 12k peak.

To confirm that the signal around 50 MHz originates from ^{59}Co and not from ^{57}Fe, the external field dependence was measured as shown in Figs. 7(a) and (b). Upon the application of external fields, the 2b peak shifts downward by −0.14 MHz/kOe, the low-frequency peak at around 50 MHz shifts upward at a higher rate of +0.7 MHz/kOe and the spectrum spreads more rapidly than the 2b spectrum. This verifies that the signal is ascribable to ^{59}Co NMR. Notably, the demagnetization effect, which becomes prominent when using a single crystal in contrast to the case when using a powdered sample, induces field-independent behavior of the resonant frequency in the low field region below ∼5 kOe, as shown in Fig. 7.

As observed here, this ^{59}Co NMR spectrum should correspond to the low-spin Co^{3+} in the octahedral coordination, because any other state of Co^{3+} in Table II cannot be assigned to such a low-frequency position. The ^{57}Fe NMR lines stay sharp in this case because Co^{3+} dopants are non-magnetic. The observed hyperfine field of ∼50 kOe corresponding to ∼50 MHz is transferred from the surrounding Fe moments. If the non-magnetic Co^{3+} existed even in the (La, Co)-codoped case, ^{59}Co-NMR should appear around ∼50 MHz, at least in the dilute doping levels.

D. (La, Co)-codoped M-type Sr ferrite $Sr_{1-x}La_xFe_{12-x}Co_xO_{19}$

1. *Low frequency region*

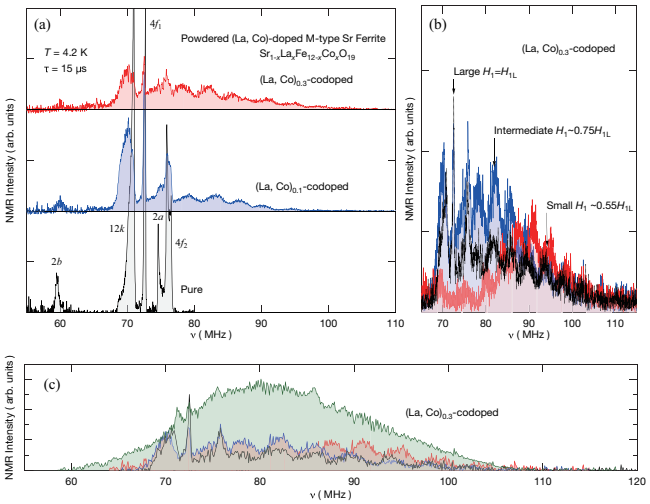

FIG. 8. (a) Zero field ^{57}Fe NMR spectra of powdered (La, Co)$_{0.1}$ and (La, Co)$_{0.3}$-codoped M-type Sr ferrite. The spectra of pure M-type Sr ferrite are shown for comparison. (b) The spectra of (La, Co)$_{0.3}$ are recorded with several magnitudes of H_1. The magnitude of H_{1L} is determined to maximize the $4f_1$-^{57}Fe signal. (c) The spectra of (La, Co)$_{0.3}$ obtained with a much reduced H_1 (roughly, < 10% of H_{1L}) is superimposed, and its magnitude is adjusted to maximize the NMR signal at ∼80 MHz.

We examine all features of the powder spectra around ^{57}Fe NMR in the (La, Co)-codoped M-type Sr ferrite. Figure 8(a) shows the ^{57}Fe NMR spectra of the powdered samples of (La, Co)-codoped M-type Sr ferrites and the pure one. In addition to the original ^{57}Fe NMR, broad spectral humps around 80 MHz appear in the spectra of (La, Co)$_{0.1}$ and (La, Co)$_{0.3}$-codoped samples, which correspond to the peaks previously reported for ^{59}Co NMR.[12] Here, the spectral envelope taken by several magnitudes of H_1, as shown in Fig. 8(b), is presumed to be the spectrum of the powdered sample of each composition. Even if the magnitude of H_1 is reduced considerably, as shown in Fig. 8(c), the high frequency spectral weight around 80–90 MHz is excited easily, and the broad spectrum fully covers the ^{57}Fe NMR spectra. At least, from Fig. 8(a), by (La, Co)-codoping, the $4f_1$ peak is found to remain nearly as sharp as it is in the case of pure M-type Sr ferrite. The 2b, 12k, and $4f_2$ peaks remain visible, but the 2a peak is indistinguishable from the surrounding ^{59}Co NMR signals.

The overlapped ^{57}Fe NMR can be observed clearly if the ^{59}Co signals are separated with the help of an external magnetic fields. As shown in Fig. 9(a), the ^{59}Co NMR spectrum is shifted largely to the high-frequency side by external fields, because of the larger $^{59}\gamma_N$, but

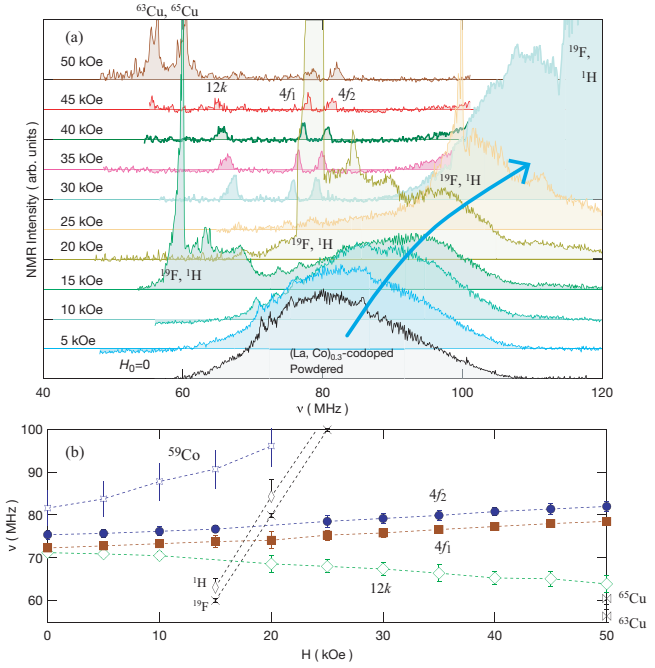

FIG. 9. External field dependence of NMR spectra of powdered (La, Co)$_{0.3}$-codoped M-type Sr ferrite sample around 80 MHz. (b) Resonant frequencies versus H_0 plot of the (La, Co)$_{0.3}$-codoped M-type Sr ferrite sample. In both plots, extrinsic NMR signals around the sample for ^{1}H, ^{19}F, and ^{63,65}Cu are tagged as well, which originate from enamel insulation, fluorocarbon polymers, and copper coil.

the ^{57}Fe NMR spectra do not move as much owing to the small $^{57}\gamma_N$. After applying $H_0 = 30$ kOe, the 12k-, 4f_1-, and 4f_2-^{57}Fe NMR peaks are visible clearly in Fig. 9(a). If the frequencies are plotted against H_0, the slopes of the 12k, 4f_1, and 4f_2 sites correspond to those of the pure M-type Sr ferrite in Fig. 4(b), but the 2a-^{57}Fe NMR peak seems to be wiped out by (La, Co)-codoping, because no frequency-decreasing peak is found between the 12k and 4f_1 peaks upon the application of a field. Here, it is emphasized that the 2a sites are strongly influenced and disappear by (La, Co)-codoping, while these 2a sites are clearly observable in the case of sorely La-doping. This is consistent with the results of a recent Mössbauer measurement of the (La, Co)-codoped system.[5] Moreover, the entire observed ^{59}Co NMR shifts to a higher frequency upon the application of external fields, which represents a positive slope, as plotted in Fig. 9(b), that is consistent with the previous NMR result.[12]

To observe the effects of (La, Co)-codoping on the Fe sites in greater detail, the single crystals' NMR spectra are compared. If the pulse condition is adjusted to maximize the 12k-Fe NMR signal, ^{57}Fe NMR-specified spectra are obtained for various (La, Co)-codoped M-type Sr ferrites, as shown in Fig. 10(a). To obtain each spectrum, a piece of single crystal is used with the domain sensitive setting of $H_1 \perp c$. As seen for the powdered sample, the single crystal data show that the 2a peak is broad-

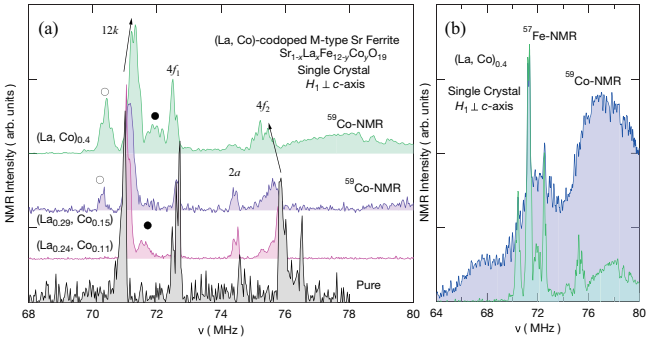

FIG. 10. (a) Frequency-swept ^{57}Fe NMR spectra for single crystals of (La$_{0.24}$, Co$_{0.11}$), (La$_{0.29}$, Co$_{0.15}$), (La, Co)$_{0.4}$-codoped, and non-doped M-type Sr ferrites under zero field with a setting of $H_1 \perp c$. The H_1 magnitude is adjusted to maximize the 12k signal. (b) Spectral difference for (La, Co)$_{0.4}$-codoped with different magnitudes of H_1: One is for the ^{57}Fe-NMR with the larger magnitude of H_1 and another is for ^{59}Co-NMR with a tiny magnitude of H_1.

ened significantly by (La, Co)$_{0.4}$-codoping. The 4f_2 peak seems to shift downward to the lower frequency side, but the 12k peak shifts upward with increasing Co in various cases of (La, Co)-codoping, although the 4f_1 peak seems to be robust in various cases of (La, Co)-codoping, where the linewidth remains sharp as well. It is noteworthy that the 12k peaks have satellite-like peaks on both sides, which are marked by (•) and (○) in Fig. 10(a). The higher satellite-like peak (•) here has been seen even in the powdered solely La-doped Sr ferrite, as shown by (↓) in Fig. 5. Probably the lower satellite peak (○) is a new peak caused by (La, Co)-codoping. As shown in Fig. 10(b), the ^{59}Co NMR signal is colossal, even in the case of a single crystal, when the magnitude of H_1 is reduced.

2. *High frequency region*

According to the recent ^{59}Co-NMR work by H. Nakamura *et al.*[15], the observed ^{59}Co NMR around 80 MHz is labeled as "S1". Moreover, "S2" around 300 MHz, "S3" around 380 MHz, and "S4" around 520 MHz are reported. Hereafter, the same labels are used for ^{59}Co-NMR. Because the last work was performed using a non-tuned NMR system specified for ferromagnets[15], it is valuable to compare the present results obtained using a conventional NMR system with an optimally tuned rf circuit. The ^{59}Co NMR signals of S2 and S3 have been successfully observed, as shown in Fig. 11 even while using a general pulsed NMR system, although S4 is out of the range of the current NMR system, of which integral intensity is reported to be less than 0.2% of the entire ^{59}Co NMR.[15]

As shown in Fig. 11(a), S2 and S3 are considerably smaller than the integral intensity of S1, which is very consistent with the results of a previous work.[15] Here, all the spectra for S1, S2 and S3 are obtained as envelops of

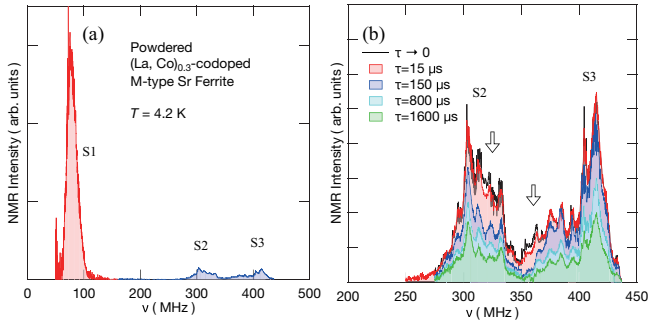

FIG. 11. (a) Zero field ^{59}Co NMR spectra of powdered polycrystalline (La, Co)$_{0.3}$-codoped M-type Sr ferrite taken with a fixed separation of τ=15 μs. ^{59}Co NMR spectra are labeled as S1, S2, and S3, respectively. (b) The magnified ^{59}Co NMR spectra of S2 and S3 in the high-frequency region. The spectra are recorded with several separations of τ=15, 150, 800, and 1600 μs. The extrapolated intensities of $\tau \rightarrow 0$ are also shown.

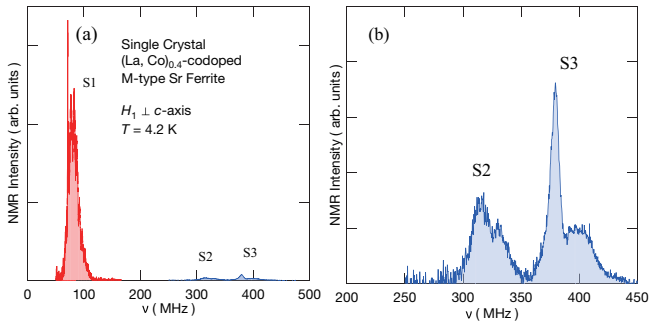

FIG. 12. (a) Zero field ^{59}Co NMR spectra of single crystal of (La, Co)$_{0.4}$-codoped M-type Sr ferrite with a setting of $H_1 \perp c$. (b) Magnified ^{59}Co NMR spectra S2 and S3 of single crystal in the high-frequency region.

their spectra taken at several H_1-magnitudes to remove certain site-dependence by H_1-enhancement factors. The separation τ dependence of S2 and S3 is shown in Fig. 11(b). Both S2 and S3 include short T_2 components, as indicated by the outlined downward arrows in Fig. 11(b), which may be ascribed to the magnetic domain walls. S2 and S3 can be observed even when using a single crystal of (La, Co)$_{0.4}$-codoped M-type Sr ferrite, as shown in Fig. 12. As discussed for ^{57}Fe NMR in Sec. III A, the ^{59}Co NMR signals may also come not from the cores of domains but from the interfacial areas of magnetic walls.

The bottom panel of Fig. 13 shows the (La, Co)-codoping dependence of S2 and S3 of M-type Sr ferrite. Both S2 and S3 exist even in the dilute doping region of (La, Co)$_{0.1}$. The spectral shape changes with the amount of (La, Co)-codoping: for example, the spectral weights are shifted from (▽) to (▼) in S2, and from (□) to (■) in S3, as shown in Fig. 13. These multi-spectral weights may imply that (La, Co) codoping causes extensive hyperfine field distribution on the Co ions.

Upon the application of an external field, S2 and S3 are

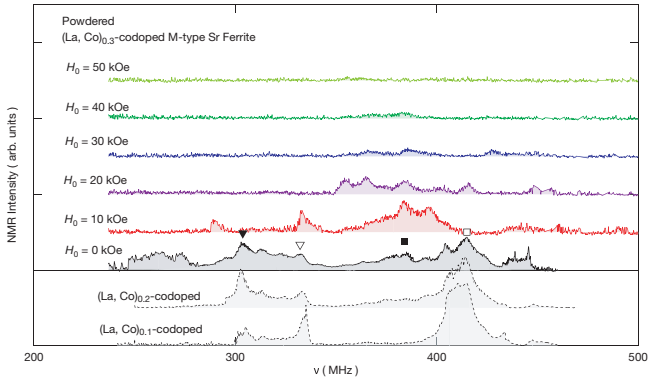

FIG. 13. Bottom panel: Zero field ^{59}Co NMR spectra of powdered (La, Co)$_{0.1}$, (La, Co)$_{0.2}$, and (La, Co)$_{0.3}$-codoped M-type Sr ferrites recorded with a fixed separation of τ=15 μs in the high-frequency region of S2 and S3. Upper panel: External field dependence of high-frequency ^{59}Co NMR spectra labeled S2 and S3, of powdered (La, Co)$_{0.3}$-codoped M-type Sr ferrite.

shifted and broadened in a complicated manner, as shown in the upper panel of Fig. 13, and then they are wiped out totally. As shown here, the doping and external field dependence suggest that S2 and S3 may contain multiple (two or more) Co sites, or there are large distributions of hyperfine fields (probably due to transferred terms). Again, it should be emphasized that S2 and S3 (and S4) are minor components of ^{59}Co NMR in (La, Co)-codoped M-type Sr ferrite. While S1 is shifted uniformly to the high-frequency side, S2 and S3 are wiped out easily upon the application of external fields.

IV. DISCUSSION

An absolutely key issue associated with ^{59}Co NMR is the assignment of the low-frequency S1 component, which corresponds to the largest number of Co ions. If this is fixed, the other assignments of S2, S3, and S4 can be determined semi-automatically. As already discussed by H. Nakamura *et al.*[15], the following assignments of S1 are considered: (i) octahedral Co^{2+} with a low-spin state of S=1/2, (ii) octahedral Co^{3+} with a low-spin (nonmagnetic) of S=0, or (iii) octahedral/tetrahedral Co^{2+} with S=3/2. (see Table II)

Indeed, M. W. Pieper *et al.*,[12] formerly adopted scenario (i). The low-spin Co^{2+} (S=1/2) ions in S1 were assumed to be at the $4f_2(\downarrow)$ sites. The octahedral low-spin Co^{2+} state of $t_{2g}^6 e_g^1$ is, however, very rare to our knowledge. One example has been reported for the spinel ferrite $FeCo_2O_4$, in which Co ions at the octahedral B sites might be partly in the low-spin Co^{2+} state.[25] Notably, single occupancy of the e_g orbitals in the low-spin Co^{2+} state leads to Jahn-Teller instability. Typically, octahedral oxygen cages are distorted easily. Therefore, scenario (i) can be ruled out because the corresponding S1 states are very stable through various doping levels.

In case (ii), there are several examples of non-magnetic Co^{3+} ions in octahedral coordination. For example, even in case of the ferromagnetic spinel compound $Co_{0.6}Fe_{0.9}Mn_{1.5}O_4$, it is argued based on the results of ^{59}Co NMR and X-ray absorption spectroscopy (XAS) that the Co dopants at the octahedral B sites are in the low-spin Co^{3+} state, although the remaining tetrahedral Co^{2+} dopants at the A sites have S=3/2.[26] In the cobalt spinel Co_3O_4, the Co^{3+} at the octahedral B site is non-magnetic[27]. In addition, octahedral non-magnetic Co^{3+} are seen in several Co oxides: $YBaCo_2O_{5.5}$,[28] $Nd_{1-x}SrCoO_3$,[29] and $Na_{0.75}CoO_2$[30]. The case (ii) is, however, incoherent because such non-magnetic Co^{3+} dopants cause ^{59}Co-NMR in the frequency range around 50 MHz, by transferred hyperfine field from the neighboring Fe moments, as shown in Sec. III C. Moreover, in the (La, Co)-codoping case, scenario (ii) means that there should be a considerable amount of divalent Fe^{2+} ions. In reality, however, the amount of Fe^{2+} ions is chemically estimated to be $x - y$ in the chemical formula of $Sr_{1-x}La_xFe_{12-y}Co_yO_{19}$ by the titration method of Ce^{4+} ions.[6] Namely in the case of $x \approx y$, Fe^{2+} ions must be very few.

Now, we can conclude that scenario (iii) is the most plausible, i.e., S1 of ^{59}Co NMR in (La, Co)-codoped M-type Sr ferrite is caused by the compensation of spin and orbital moments. If most Co ions are assumed to be divalent in the case of (La, Co)-codoping, the S=3/2 state is the most common in both octahedral and tetragonal coordinations, although tetrahedral Co^{2+} is an orbital singlet in the CEF ground state. A. Morel *et al.*,[31] assigned the S1 spectrum (reported by M. W. Pieper *et al.*,[12]) to high-spin Co^{2+} at the octahedral $4f_2$ sites assuming the presence of an unquenched orbital moment. Similarly, a large orbital moment $m_l \sim 0.6\ \mu_B$ was detected in the related spinel compound $CoFe_2O_4$ by using magnetic Compton scattering.[32]

By considering intra-atomic spin and orbital terms alone, the hyperfine field, H_{hf}, can be written as $H_{hf} = \alpha m_s + \beta m_l$, where m_s (m_l) is the spin (orbital) moment, and α (β) is a spin (orbital) hyperfine coupling constant. The value of α is known to be about -130 to -120 kOe/μ_B, and the estimated values of β for high spin Co^{2+} in several typical compounds are about +515–720 kOe/μ_B for CoO[33], +650–750 kOe/μ_B for $CoCl_2{\cdot}2H_2O$[34] and $CsCoCl_3$[35], and +640–650 kOe/μ_B for RCo_5 (R=Y, Sm)[36]. Because α and β have negative and positive signs, respectively, if m_l remains unquenched considerably, compensation occurs such that H_{hf} would become small even in the high-spin state. In addition to these examples, in the cubic spinel $CoCr_2O_4$, even the tetrahedral Co^{2+} ion, whose CEF ground state is considered to be an orbital singlet, shows low-frequency NMR around 55 MHz resulting from the compensation by the orbital contribution[37], as discussed later.

S1, S2, and S3 have been observed almost identically at several doping levels of ($La_{0.24\sim0.3}$, $Co_{0.11\sim0.15}$) to (La, Co)$_{0.1\sim0.4}$. Therefore, they can be assigned to divalent

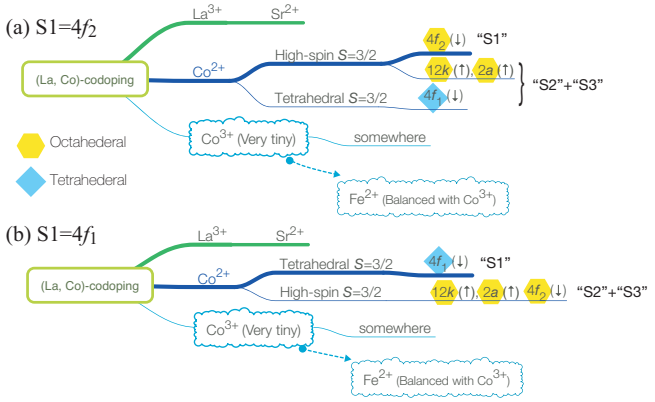

FIG. 14. Summary views of charge and spin states, and doping sites in (La, Co)-codoped M-type Sr ferrite. Two cases are illustrated: main substitutions of Co^{2+} occur at (a) octahedral $4f_2$ sites, and (b) tetrahedral $4f_1$, which should correspond to S1.

Co^{2+} ions, not to trivalent Co^{3+}, because unbalanced doping does not affect S1, S2, and S3 although the ratio of Co^{3+} varies. Here, the very minor high-spin Co^{3+} (S=2) can be assigned to the reported minimal fraction of S4, which is less than 0.2% in the ($La_{0.289}$, $Co_{0.152}$)-codoped sample[15]. As a result, it is quite natural that Fe^{2+} NMR signal would be very weak in the (La, Co)-codoped system, corresponding to the amount of Co^{3+}.

As discussed above, in scenario (iii), in principle, it is allowable that S1 contains several Co contributions on the various Fe sites, if the assignment can explain the result that ^{59}Co-NMR frequencies increased with increasing external fields. However, it is unlikely that a common balance of αm_s and βm_l for Co ions on the various Fe sites was realized accidentally. Therefore, it is practical to consider that S1 can be ascribed for the most part to Co^{2+} substitutions at one particular Fe site.

On the other hand, the results of a macroscopic magnetization study using single crystals of (La, Co)-codoped Sr ferrites[7,8], show that the saturation moments are certainly increased by $\sim$0.4 μ_B/(f.u.) for x = 0.4 from 20 μ_B/(f.u.) in the non-doped case. If most of the Co^{2+} having about 3–3.5 μ_B, including orbital moments, were to be substituted only for the minority spin sites ($\downarrow$), 0.6–0.8 μ_B/(f.u.) could be expected, which is larger than the experimental value. This means that the Co^{2+} substitutions are distributed across the minority and majority spin sites, but more than half of the substitutions occur at the minority spin sites, which contribute to S1. Consequently, in terms of the assignment of S1, there are two possibilities. Co^{2+} could occupy either the octahedral $4f_2(\downarrow)$ or the tetrahedral $4f_1(\downarrow)$ site.

Presumably, as A. Morel *et al.*, discussed[31], one may think that the case of $4f_2(\downarrow)$ is preferable because the high-spin Co^{2+} (S=3/2) configuration of $t_{2g}^5 e_g^2$ in octahedral CEF yields an unquenched orbital moment, and because the CEF ground state of tetrahedral Co^{2+} is an orbital singlet for the $e_g^4 t_{2g}^3$ configuration. In this case,

the hyperfine field $|H_{\rm hf}(4f_2)| \sim 80$ kOe would be produced by a rough sum of $\alpha m_s \sim -100$ (kOe/$\mu_{\rm B}$) $\times$ 3 $\mu_{\rm B}$ and $\beta m_l \sim +600$ (kOe/$\mu_{\rm B}$)$\times m_l$. A relatively large transferred hyperfine field $H_{\rm tr}$ from the neighboring Fe^{3+} spins of 5 $\mu_{\rm B}$ should be added to $H_{\rm hf}$, which is estimated to be roughly $\sim$100 kOe for each vacant Fe site. Because S1 shifts to the high-frequency side upon the application of external field, $H_{\rm hf}$ would be negative. Assuming the Co spins follow the same direction as that of the $4f_2$-Fe spins, the estimated value of m_l is roughly 0.2–0.5 $\mu_{\rm B}$, which is slightly smaller than that expected from the orbital triplet state of $L = 1$.

Then, assuming the main Co^{2+} ions might be doped into the $4f_2$-Fe sites, S2 and S3 should be assigned as follows. Fractional substitutions of Co^{2+} to the similar octahedral $12k$ and $2a$ sites should occur, because there is no specific reason to exclude this possibility at this point. Indeed, the high-spin Co^{2+} states with octahedral coordination in the case of Co ferrite $CoFe_2O_4$[38,39] are seen in the similar frequency range as S2 and S3. In the literature[38], the origin of the distributions of hyperfine fields is ascribed to sites-to-sites differences of transferred hyperfine fields. This appears to be consistent with the fact that S2 and S3 suggest a distribution of hyperfine fields, as shown in Fig. 13. Perhaps, if only the CEF ground state is assumed, the tetrahedral Co^{2+} (S=3/2), too, might be assigned to S3, namely, a small part of Co^{2+} might go to the $4f_1(\downarrow)$ sites. Because the on-site hyperfine field of the spin-only 3 $\mu_{\rm B}$ of tetrahedral Co^{2+} can be estimated to be roughly -300 kOe, this might appear in the frequency ranges of S2 or S3, in addition to the transferred field with an order of $\sim$100 kOe from the neighboring Fe^{3+} spins.

Let us summarize as Fig. 14(a). In this case, the high-spin Co^{2+} ions on the octahedral $12k$ and $2a$ lead to the generation of S2 and S3, of which frequencies are centered at $\sim$350 MHz, quite far from the S1 range of $\sim$80 MHz to the similarly octahedral $4f_2$. In the case of S2 and S3, m_l is estimated to be 0.9–1.3 $\mu_{\rm B}$, which appears to be appropriate for the state $L = 1$. Notably, in the (La, Co)-codoped Sr ferrite, the $2a$ coordination is the least distorted octahedron, and $12k$'s and $4f_2$'s octahedral coordinations are distorted comparably which have relatively-larger quadrupolar shifts in ^{57}Fe-Mössbauer experiment[3]. Therefore, it is quite unnatural that $4f_2$-Co^{2+} would be singular to have a smaller orbital moment. Indeed, a very recent ab-initio calculation[40] to compare the XAS in the partial fluorescence yield mode (PFY-XAS) at the Co-K edge indicates the preferential $4f_1$ substitutions, and the higher potential energies of Co occupancies in $4f_2$ and $2b$, which are $\sim$1 eV higher than those in $4f_1$, $12k$, and $2a$. Accordingly, the assumption of major $4f_2$-doping is considered inappropriate.

We now turn to the alternative $4f_1(\downarrow)$ possibility for the assignment of S1. As already noted, the CEF ground state of tetrahedral Co^{2+} (S=3/2) is an orbital singlet. In Co oxides, however, the tetrahedral CEF energy splitting between e_g and t_{2g} is considerably smaller than that in octahedral CEF. For example, in the cobalt spinel Co_3O_4, tetrahedral Δ_t of $\sim$4000–5000 K, and the octahedral Δ_o of $\sim$20000–50000 K are reported[41–43]. In the first approximation, $m_l = 0$ for this orbital singlet, but the orbital quenching is lifted partially by the second-perturbation with the first excited CEF state owing to spin-orbit interaction λLS, whose energy scale is known to be $\lambda \sim$200 K for Co^{2+}. Very recently, the tetrahedral Co^{2+} in $CoCr_2O_4$ has been found to carry such an orbital moment of $\sim$0.2 $\mu_{\rm B}$ by means of XMCD and resonant soft X-ray diffraction techniques.[44] The hyperfine field $H_{\rm hf}({\rm SO}) = \xi m_s$ caused by this perturbation approximates to $2\mu_{\rm B}k\langle r^{-3}\rangle_d(g-2)m_s$, where k is an orbital reduction factor (~ 0.8), $\langle r^{-3}\rangle_d$ is the average of r^{-3} over $3d$ electrons, and g is the effective g-factor. For the tetrahedral Co^{2+} in Co_3O_4[43], it is estimated to be $\xi \sim +85$ kOe/$\mu_{\rm B}$, and a similar value is given for $CoCr_2O_4$ as well[37].

Thus, the $4f_1$-Co^{2+} can be naturally assigned to S1, because $H_{\rm hf}(4f_1) \sim -80$ kOe is compatible with $(\alpha + \xi)m_s$, if $\alpha \sim -100$ (kOe/$\mu_{\rm B}$) and $\xi \sim +70$–80 (kOe/$\mu_{\rm B}$) are assumed. Then, the octahedral high-spin Co^{2+} at the $12k$, $2a$, and $4f_2$ sites can be applied to the assignments of S2 and S3, as discussed above. Thus, these assignments of S1, S2, and S3, as shown in Fig. 14(b), become fully coherent.

As seen in Fig. 13, S2 and S3 show hyperfine field distributions, which are similar to Co ferrite[39], and are caused by local environmental effects of the other Co dopants. Simultaneously, every high-spin Co^{2+} ion possesses an unquenched orbital moment that is roughly close to $m_l \sim 1$ $\mu_{\rm B}$ with $m_s \sim 3$ $\mu_{\rm B}$, which should induce local magnetic anisotropy. Because the external field dependence shown in Fig. 13 was recorded using a powdered specimen, the extreme-uniaxial anisotropy of the hyperfine field would cause an anisotropic resonance shift, i.e., each resonance in S2 and S3 would be broadened inhomogeneously and abruptly upon the application of an external field. Such an inhomogeneous broadening must be more increased if the direction of magnetic anisotropy for Co^{2+} is different from sites to sites, i.e., it is still possible that uniaxial anisotropy on the $12k$, $2a$, and $4f_2$ may not be always along the c axis.

Even the tetrahedral $4f_1$-Co^{2+} ions, which are assigned to S1, should cause uniaxial magnetic anisotropy as well by the partially unquenched orbital moment. Notably, the inhomogeneous broadening seen in S2 and S3 is much smaller in S1, because of its smaller orbital moment and/or its uniform local magnetic anisotropy through the $4f_1$ sites. Perhaps, the magnetic anisotropy increased by (La, Co)-codoping[2] might be owing to the relative ratio of Co^{2+} amount occupied at the specific sites. Further study to reveal the sites-to-sites anisotropies of Co^{2+} should be extremely promising to give a clue to improve the bulk magnetic anisotropy.

Finally, we check the consistency between these assignments and the ^{57}Fe NMR results. Even though the Co^{2+} ions are mainly doped into the $4f_1$ sites, (and there

is slight doping of Co^{2+} at the $12k$, $2a$, and $4f_2$ sites), most Fe^{3+} sites are far from the (La, Co)-dopants, at most $Co_{0.4}$, with respect to Fe_{12} per (f.u.). The substituted Co^{2+} ions lead to distributions of transferred hyperfine fields, which influence the nearest Fe sites. Notably, the on-site hyperfine fields of ^{57}Fe cannot be influenced by Co doping. The Co^{2+} ions at the $4f_1$ sites change the local hyperfine fields at the neighboring $12k$ sites, leading to the emergence of the satellite-like peaks, as shown in Figs. 8(a) and 10(a). Next, the $2a$ ^{57}Fe-NMR is wiped out easily by a large distribution of transferred hyperfine fields from Fe^{3+} and Co^{2+} at the surrounding $12k(\uparrow)$ and $4f_1(\downarrow)$. Indeed, the distance from the nearest-neighboring $12k$ sites to the $2a$ sites is about 3.0 Å, which is the shortest among the other Fe sites ranging from 3.3 Å to 3.7 Å for the respective nearest neighbors, except for the Fe-Fe distances of 2.7–3.0 Å between the two $4f_2$ and two $12k$ sites, respectively. By contrast, the $4f_1$ sites are on average 3.5–3.7 Å from the other Fe sites. Therefore, it is reasonable that the $4f_1$ spectrum remains sharp in the (La, Co)-codoped system.

V. CONCLUSION

Our comprehensive NMR study concluded that Co^{2+} ions are substituted mainly at tetrahedral $4f_1$ sites, and that the remaining fractional Co^{2+} ions are distributed among the octahedral $12k$ and $2a$ Fe sites in (La, Co)-codoped M-type Sr ferrite. To a considerable degree, the charge compensation between La^{3+} and Co^{2+} works in the equal (La, Co)-codoped case. The partially lifted orbital moment due to spin-orbit interaction is an important feature of the tetrahedral Co^{2+} state. Meanwhile, the minor octahedral Co^{2+} ions have unquenched orbital moments. A very recent Mössbauer study using the same batches of single crystals drew a similar conclusion[45]. Moreover, previous and recent works using ND, EXAFS, XMCD, and energy-dispersive X-ray spectroscopy (EDXS)[10,46] have yielded a similar conclusion as well.

Because the contribution of S4 corresponding to Co^{3+} is less than 0.2% in the unbalanced ($La_{0.289}$, $Co_{0.152}$)-codoped sample[15], the amounts of Co^{3+} and Fe^{2+} should be smaller in the equally codoped $(La, Co)_{0.4}$ case. Considering a recent investigation[8] suggests that Fe^{2+} states would emerge with further codoping of $x > 0.4$ and y=0.4 in $Sr_{1-x}La_xFe_{12-y}Co_yO_{19}$, Fe^{2+} NMR search of such a sample is an avenue for future research on this issue.

The presence of partially lifted and unquenched orbital moments in Co^{2+} is probably the reason why (La, Co)-cosubstitution improves magnetic performance parameters, such as saturation magnetization M_s, coercive force H_c, and anisotropy field H_A. The orbital moment improves magnetic anisotropy energy, as theoretically predicted in the case of Co ferrite[47] more than half a century ago.

ACKNOWLEDGMENTS

We thank H. Ikeno, S. Ikeda, H. Kobayashi, and Y. Takahashi for valuable discussions. We also thank F. Ronning for a critical reading of the manuscript. This research was supported by Japan Science and Technology Agency (JST) under the Collaborative Research Based on Industrial Demand "High Performance Magnets: Towards Innovative Development of Next Generation Magnets" (Grant Numbers 11103672 and 14532720).

* sakai.hironori@jaea.go.jp
† nakamura.hiroyuki.2w@kyoto-u.ac.jp

[1] R. C. Pullar, Progress in Materials Science **57**, 1191 (2012).
[2] K. Iida, Y. Minachi, K. Masuzawa, M. Kawakami, H. Nishio, and H. Taguchi, Journal of the Magnetics Society of Japan **23**, 1093 (1999).
[3] G. Wiesinger, M. Müller, R. Grössinger, M. Pieper, A. Morel, F. Kools, P. Tenaud, J. M. L. Breton, and J. Kreisel, physica status solidi (a) **189**, 499 (2002).
[4] L. Lechevallier, J. M. L. Breton, J. Teillet, A. Morel, F. Kools, and P. Tenaud, Physica B **327**, 135 (2003).
[5] N. Nagasawa, S. Ikeda, A. Shimoda, T. Waki, Y. Tabata, H. Nakamura, and H. Kobayashi, Hyperfine Interactions **237**, 39 (2016).
[6] N. Langhof and M. Göbbels, J. Solid State Chem. **182**, 2725 (2009).
[7] A. Shimoda, K. Takao, K. Uji, T. Waki, Y. Tabata, and H. Nakamura, J. Solid State Chem. **239**, 153 (2016).
[8] H. Ueda, Y. Tanioku, C. Michioka, and K. Yoshimura, Phys. Rev. B **95**, 224421 (2017).
[9] A. Morel, J. M. L. Breton, J. Kreisel, G. Wiesinger, F. Kools, and P. Tenaud, J. Magn. Magn. Mater. **242-245**, 1405 (2002).
[10] Y. Kobayashi, E. Oda, T. Nishiuchi, and T. Nakagawa, Journal of the Ceramic Society of Japan **119**, 285 (2011).
[11] J. M. L. Breton, G. Wiesinger, C. T. Blanco, O. Isnard, J. Teillet, R. Grössinger, A. Morel, F. Kools, and P. Tenaud, in *Ferrites : Proceedings of the ICF 8*, edited by M. Abe and Y. Yamazaki (Japan Society of Powder and Powder Metallurgy, 2000) p. 199.
[12] M. W. Pieper, F. Kools, and A. Morel, Phys. Rev. B **65**, 184402 (2002).
[13] J. Töpfer, D. Seifert, J.-M. L. Breton, F. Langenhorst, V. Chlan, K. Kouřil, and H. Štěpánková, J. Solid State. Chem. **226**, 133 (2015).
[14] H. Ikeno, Physica B **532**, 20 (2018).
[15] H. Nakamura, A. Shimoda, T. Waki, Y. Tabata, and C. Mény, J. Phys. :Condens. Matter **28**, 346002 (2016).
[16] K. Kouřil, *Local Structure of Hexagonal Ferrites Studied by NMR*, Ph.D. thesis, Department of Low Temperature Physics, Faculty of Mathematics and Physics, Charles Univ. in Prague (2013).
[17] H. Morishita, A. Amano, H. Ueda, C. Michioka, and K. Yoshimura, J. Jpn. Soc. Powder Powder Metallurgy **61**

Suppl., S64 (2014).
[18] R. L. Streever, Phys. Rev. **186**, 285 (1969).
[19] K. Hareyama, K. Kohn, and K. Uematsu, J. Phys. Soc. Jpn. **29**, 791 (1970).
[20] H. Štěpánková, J. Englich, P. Novák, B. Sedlák, and M. Pfeffer, Hyperfine Interactions **50**, 639 (1989).
[21] M. W. Pieper, A. Morel, and F. Kools, J. Magn. Magn. Mater. **242-245**, 1408 (2002).
[22] M. Kontani and J. Itoh, J. Phys. Soc. Jpn. **22**, 345 (1967).
[23] H. Štěpánková, J. Englich, P. Novák, and H. Lütgemeier, J. Magn. Magn. Mater. **104-107**, 409 (1992).
[24] M. Küpferling, R. Grössinger, M. W. Pieper, G. Wiesinger, H. Michor, C. Ritter, and F. Kubel, Phys. Rev. B **73**, 144408 (2006).
[25] N. Kita, N. Shibuichi, and S. Sasaki, J. Synchrotron Rad. **8**, 446 (2001).
[26] H. Jung, S.-J. Lee, M. Song, S. Lee, H. J. Lee, D. H. Kim, J.-S. Kang, C. L. Zhang, and S.-W. Cheong, New J. Phys. **11**, 043008 (2009).
[27] K. Miyatani, K. Kohn, H. Kamimura, and S. Iida, J. Phys. Soc. Jpn. **21**, 464 (1966).
[28] M. Itoh, Y. Nawata, T. Kiyama, D. Akahoshi, N. Fujiwara, and Y. Ueda, Physica B **329-333**, 751 (2003).
[29] A. Ghoshray, B. Bandyopadhyay, K. Ghoshray, V. Morchshakov, K. Bärner, I. O. Troyanchuk, H. Nakamura, T. Kohara, G. Y. Liu, and G. H. Rao, Phys. Rev. B **69**, 064424 (2004).
[30] M. H. Julien, C. de Vaulx, H. Mayaffre, C. Berthier, M. Horvatić, V. Simonet, J. Wooldridge, G. Balakrishnan, M. R. Lees, D. P. Chen, C. T. Lin, and P. Lejay, Phys. Rev. Lett. **100**, 096405 (2008).
[31] A. Morel, P. Tenaud, F. Kools, and J. M. L. Breton, in *Proceedings of the International Conference on Ferrites (ICF-9)*, edited by R. F. Soohoo (Wiley-Blackwell, 2005) p. 339.
[32] H. S. Mund, S. Tiwari, J. Sahariya, M. Itou, Y. Sakurai, and B. L. Ahuja, J. Appl. Phys. **110**, 073914 (2011).
[33] K. Okada and H. Yasuoka, J. Phys. Soc. Jpn. **43**, 34 (1977).
[34] H. Nishihara, H. Yasuoka, and A. Hirai, J. Phys. Soc. Jpn. **32**, 1135 (1972).
[35] T. Kubo, K. Adachi, M. Mekata, and A. Hirai, Solid State Communications **29**, 553 (1979).
[36] R. L. Streever, Phys. Rev. B **19**, 2704 (1979).
[37] T. Tsuda, A. Hirai, and H. Abe, Phys. Lett. **26A**, 463 (1968).
[38] T. Nishikubo and K. Motizuki, J. Phys. Soc. Jpn. **17**, 871 (1962).
[39] T. Tsuda, K. Okada, and H. Yasuoka, J. Phys. Soc. Jpn. **37**, 1713 (1974).
[40] H. Ikeno, *Privete Communication*.
[41] P. Cossee and A. E. van Arkel, J. Phys. Chem. Solids **15**, 1 (1960).
[42] N. Mironova, V. Skvortsova, and U. Ulmanis, Solid State Communications **91**, 731 (1994).
[43] T. Fukai, Y. Furukawa, S. Wada, and K. Miyatani, J. Phys. Soc. Jpn. **65**, 4067 (1996).
[44] Y. W. Windsor, C. Piamonteze, M. Ramakrishnan, A. Scaramucci, L. Rettig, J. A. Huever, E. M. Bothschafter, N. S. Bingham, A. Alberca, S. R. V. Avula, B. Noheda, and U. Staub, Phys. Rev. B **95**, 224413 (2017).
[45] M. Oura, N. Nagasawa, S. Ikeda, A. Shimoda, T. Waki, Y. Tabata, H. Nakamura, N. Hiraoka, and H. Kobayashi, Journal of Applied Physics **123**, 033907 (2018).
[46] M. Ohtsuka, S. Muto, K. Tatsumi, Y. Kobayashi, and T. Kawata, Microscopy **65**, 127 (2016).
[47] M. Tachiki, Prog. Theor. Phys. **23**, 1055 (1960).